Implementation of Modified Ensemble and Unscented Kalman Filters for Diving Trajectory Estimation of Remote Operated Vehicles

Teguh Herlambang
Department of Information System, Universitas Nahdlatul Ulama Surabaya, Indonesia | Center for Data and Business Intelligence, Universitas Nahdlatul Ulama Surabaya, Indonesia
teguh@unusa.ac.id

Rachman Sinatriya Marjianto
Department of Engineering, Faculty of Vocational, Universitas Airlangga, Indonesia
rachmansinatriya@vokasi.unair.ac.id (corresponding author)

Puguh Triwinanto
National Research and Innovation Agency, Indonesia
pugu001 @brin.go.id

Zuraini Othman
Department of Diploma Studies, Fakulti Teknologi Maklumat dan Komunikasi, Universiti Teknikal Malaysia Melaka, Malaysia
zuraini@utem.edu.my

Mohd. Sanusi Azmi
Department of Software Engineering, Fakulti Teknologi Maklumat dan Komunikasi, Universiti Teknikal Malaysia Melaka, Malaysia
sanusi@utem.edu.my

Nuzulha Khilwani Ibrahim
Department of Diploma Studies, Fakulti Teknologi Maklumat dan Komunikasi, Universiti Teknikal Malaysia Melaka, Malaysia
nuzulha@utem.edu.my

Nor Mas Aina Md. Bohari
Department of Diploma Studies, Fakulti Teknologi Maklumat dan Komunikasi, Universiti Teknikal Malaysia Melaka, Malaysia
aina@utem.edu.my

Mohammad Soleh
Department of Business, Faculty of Vocational, Universitas Airlangga, Indonesia
m.soleh@vokasi.unair.ac.id

Received: 16 August 2025 | Revised: 1 October 2025 and 10 October 2025 | Accepted: 15 October 2025

 DOI: https://doi.org/10.48084/etasr.14117

ABSTRACT

Remotely Operated Vehicles (ROVs) are underwater vehicle widely researched, developed, and utilized to perform various tasks. The primary functions of ROVs include coral reef exploration, oil refinery inspection, underwater monitoring, and sea accident rescue operations. The ROV typically has six Degrees

of Freedom (DoFs), consisting of a combination of translational and rotational motions. To ensure that the ROV moves according to a predetermined trajectory without unwanted rotation or roll, a reliable navigation and position estimation system is required. Several position estimation methods have been proven effective for ROV applications. Among these, the Ensemble Kalman Filter (EnKF) and the Unscented Kalman Filter (UKF) are recognized for their reliability. In this study, a modified version of the EnKF, known as the Square Root Ensemble Kalman Filter (SR-EnKF), is compared with the UKF method. Simulation results indicate that the SR-EnKF provides higher accuracy than the UKF, achieving approximately 99.8% accuracy compared to 99.6% obtained with the UKF.

Keywords-estimation; ROV; SR-EnKF; Trajectory; UKF

I. INTRODUCTION

Remotely Operated Vehicles (ROVs) play a vital role in underwater operations, as they are remotely controlled vehicles used for a wide range of applications — from scientific research and industrial operations to national defense and security systems [1, 2]. ROVs are also widely utilized as identification tools in the evacuation of accident victims at sea [3]. The environment navigated by ROVs is among the most challenging, as they must operate under various major disturbances [4]. These disturbances include strong currents, low temperatures, and high pressures, which require the ROV to maintain accurate tracking of its predetermined trajectory. The ROV's motion system consists of six Degrees of Freedom (6-DoF), for three translational and three rotational motions [5]. In the mathematical model of the ROV motion system, hydrodynamic coefficients significantly influence both translational and rotational behaviors [6]. In ROV development, the integration of the motion system with navigation and control systems is crucial to ensure optimal performance and precise trajectory tracking with minimal errors. The continuous advancement of technology in this field provides opportunities to enhance ROV capabilities. During operation, the ROV requires a navigation system capable of accurate trajectory estimation to determine whether it is moving forward, turning, or diving [7]. The accuracy of trajectory estimation is instrumental to successful operation, while the reliability of the navigation system is essential to prevent accidents and avoid damage to ROV [8]. This study begins by modeling the 6-DoF motion equations. Subsequently, a position estimation method is applied to determine the ROV's motion while diving underwater. Previous studies have implemented several position or motion estimation methods for unmanned underwater vehicles, including the Particle Filter [9], Extended Kalman Filter (EKF) [10], Square Root Ensemble Kalman Filter (SR-EnKF) [11], H-Infinity Method [12], Ensemble Kalman Filter (EnKF) [13], Particle Swarm Optimization (PSO) [14], and Unscented Kalman Filter (UKF) [15]. Since the Kalman Filter and its variants are known for their robustness in estimation studies, this research also references prior works [16] and [17]. Among the aforementioned methods, the SR-EnKF and UKF are particularly suitable for motion system equations that involve nonlinear models. Therefore, this study aims to compare the performance of diving and turning motion estimation in ROVs using the SR-EnKF and UKF methods.

Previous studies have extensively employed the UKF for nonlinear state estimation in autonomous and remotely operated vehicles, demonstrating its effectiveness in handling nonlinear underwater dynamics [X, Y]. Other research has explored EnKFs in oceanographic and atmospheric applications, but their use in underwater vehicle trajectory estimation remains limited. To the best of our knowledge, no prior study has explicitly investigated the Square-Root Ensemble Kalman Filter (SR-EnKF) for 6-DoF ROV dynamics. The novelty of this work lies in the application and evaluation of the SR-EnKF with square-root updates for ROV trajectory estimation, which offers improved covariance stability and accuracy compared to conventional UKF. By providing a direct comparison between the SR-EnKF and UKF under identical models and noise assumptions, this study advances the state of the art and clarifies the trade-off between estimation accuracy and computational complexity for practical underwater navigation.

II. RESEARCH METHOD

A. The 6-DoF Remotely Operated Vehicle

This study employs an ROV with a length of 900 mm and a width of 300 mm. The ROV's motion system is modelled with six DoFs, as described by (1)–(6). These equations serve as the fundamental platform for implementing the UKF and SR-EnKF algorithms. The geometric profile and specifications of the ROV utilized in this research are presented in Figure 1 and Table I [3].

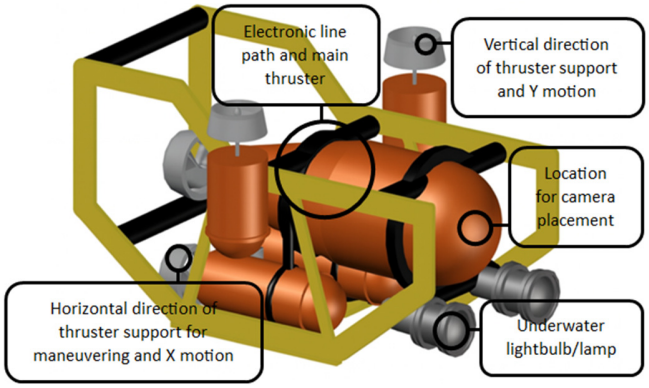

Fig. 1. ROV profile.

TABLE I. NOTATION OF ROV MOTION AXES

DoF	Translational and rotational	Force/ Moment	Linear and angular velocity	Position/ Euler angle
1	Surge	X	U	x
2	Sway	Y	V	y
3	Heave	Z	W	z
4	Roll	K	P	$\emptyset$
5	Pitch	M	Q	θ
6	Yaw	N	R	

TABLE II. ROV SPESIFICATIONS

Parameter	Description
Weight	15 Kg
Length	900 mm
Controller	Wired Control ArduSUB with joystick
Camera	TTL Camera
Battery	11.8 V Li Po 5200 mAh
Material	Carbon fiber
Main Propulsion	T200 Motor Thruster including the propeller
Maneuver Propulsion	T200 Motor Thruster including the propeller
Service Speed	1.6 knots
Operational depth	5 - 10 m

Regarding the dynamics of the ROV, there are external forces influencing the movements as follows:

$$\tau = \tau_{hidrostatic} + \tau_{addedmass} + \tau_{drag} + \tau_{lift} + \tau_{control} \quad (1)$$

$$\eta = [\eta_1^T, \eta_2^T]^T, \eta_1 = [x, y, z]^T, \eta_2 = [\emptyset, \theta, \Psi]^T$$

$$v = [v_1^T, v_2^T]^T, v_1 = [u, v, w]^T, v_2 = [p, q, r]^T \quad (2)$$

$$\tau = [\tau_1^T, \tau_2^T]^T, \tau_1 = [X, Y, Z]^T, \tau_2 = [K, M, N]^T$$

The ROV specifications in Table II are used as a data platform in a navigation and guidance system with two movements, rotational and translational. This study focused on the diving motion only so as to observe just three types of motions, i.e. surge, heave, and pitch. The motion equations are [3]:

Surge:

$$m[\dot{u} - vr + wq - x_G(q^2 + r^2) + y_G + z_G(pr + \dot{q})] \approx X \quad (3)$$

Sway:

$$m[\dot{v} - wp + ur - y_G(r^2 + p^2) + z_G(qr - \dot{p}) + x_G(pq + \dot{r})] \approx Y \quad (4)$$

Heave:

$$m[\dot{w} - uq + vp - z_G(p^2 + q^2) + x_G(rp - \dot{q}) + y_G(rq + \dot{p})] \approx Z \quad (5)$$

Roll:

$$I_x\dot{p} + (I_z - I_y)qr + m[y_G(\dot{w} - uq + vp) - z_G(\dot{v} - wp + ur)] \approx K \quad (6)$$

Pitch:

$$I_y\dot{q} + (I_x - I_z)rp + m[z_G(\dot{u} - vr + wq) - x_G(\dot{w} - uq + vp)] \approx M \quad (7)$$

Yaw:

$$I_z\dot{r} + (I_y - I_z)pq + m[x_G(\dot{v} - wp + ur) - y_G(\dot{u} - vr + wq)] \approx N \quad (8)$$

The above equation can be written in a more concise form:

$$M_{RB}\dot{v} + C_{RB}(v)v = \tau \quad (9)$$

$$M_{RB} = \begin{bmatrix} mI_{3\times3} & -mS(r_G) \\ mS(r_G) & I_o \end{bmatrix} = \begin{bmatrix} m & 0 & 0 & 0 & mz_G & -my_G \\ 0 & m & 0 & -mz_G & 0 & mx_G \\ 0 & 0 & m & my_G & -mx_G & 0 \\ 0 & -mz_G & my_G & I_{xx} & -I_{xy} & -I_{xz} \\ mz_G & 0 & -mx_G & -I_{yx} & I_{yy} & -I_{yz} \\ -my_G & mx_G & 0 & -I_{zx} & -I_{zy} & I_{zz} \end{bmatrix} \quad (10)$$

where $v = [u, v, w, p, q, r]^T$ contains the vectors of linear and angular velocity, $\tau = [X, Y, Z, K, M, N]^T$ represents the external force and moment acting on the ROV, M_{RB} is the inertia matrix, and C_{RB} is the Coriolis and centripetal matrix, $I3x3$ represents a 3×3 dentity matrix, and $S(.)$ represents a 3×3 symmetric skew matrix, such as the one shown in (11):

$$S(r_G) = -S^T(r_G) = \begin{bmatrix} 0 & -z_G & y_G \\ z_G & 0 & -x_G \\ -y_G & x_G & 0 \end{bmatrix} \quad (11)$$

The $C_{RB}(v)$ matrix usually has a skew symmetric form, i.e.: $C_{RB} = -C_{RB}^T$:

$$C_{RB}(v) = \begin{bmatrix} 0_{3\times3} & -mS(v_1) - mS(v_2)S(r_G) \\ -mS(v_1) + mS(r_G)S(v_2) & -S(I_0v_2) \end{bmatrix} \quad (12)$$

B. Unscented Kalman Filter and Square Root Ensemble Kalman Filter

The UKF has a high accuracy regarding the motion estimation of nonlinear models [1] (Figure 2).

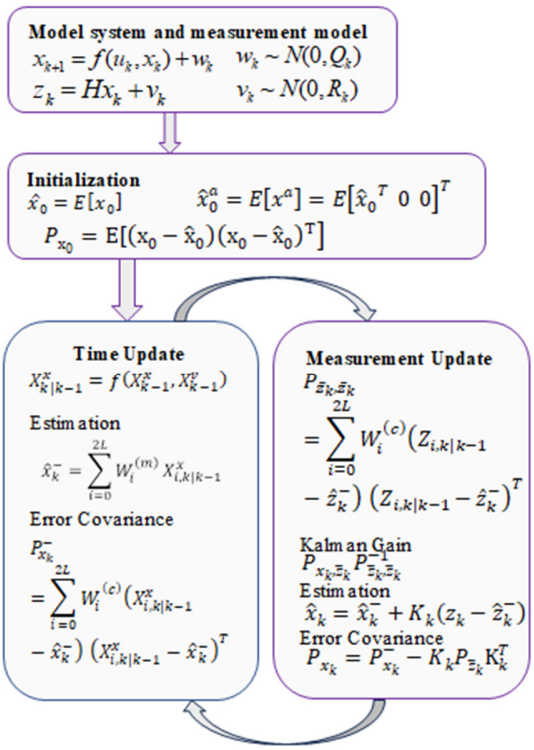

Fig. 2. Flow of the UKF.

The EnKF-SR algorithm is a developed modification of the EnKF method by adding square roots to the correction stage [10], as shown in Figure 3.

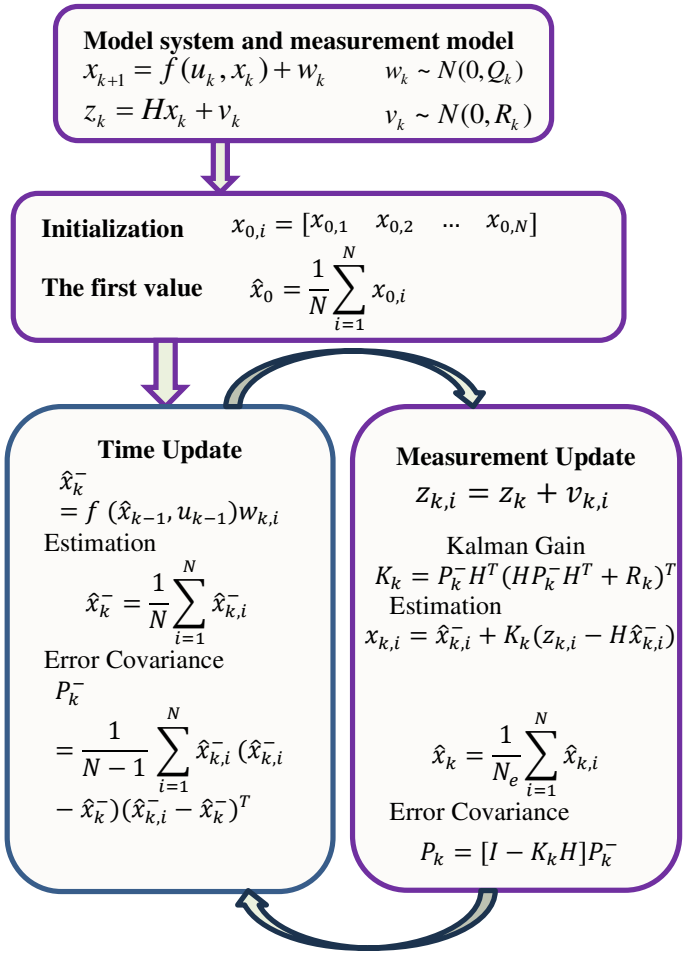

Fig. 3. Flow of the SR-EnKF.

III. RESULTS AND DISCUSSION

A. Simulation Results

Two simulations were carried out in order to compare the two methods with two different ensemble size, 100 and 300. The simulations use turning and diving trajectories, in which the ROV is required to move along the predetermined trajectory with the help of the UKF and EnKF-SR algorithms. Simulations were conducted in calm water conditions, so the disturbance value was close to 0. Simulation results by generating 100 ensembles can be seen in Figures 4 and 5.

Figure 6 shows the simulation results of the ROV movement (moving diving, and turning) in the *XYZ* plane. The resulting error in the *XY* plane is 0.11% for the SR-EnKF method and 0.12% for the UKF method. The error generated by the *XY* plane is affected by the error in the *X* position, *Y* position, and *Z* position. In Table III, it can be seen that the *X*, *Y*, and *Z* position errors of the SR-EnKF method are smaller than those of the UKF method. The position error of both methods is small due to the small RMSE of each DoF.

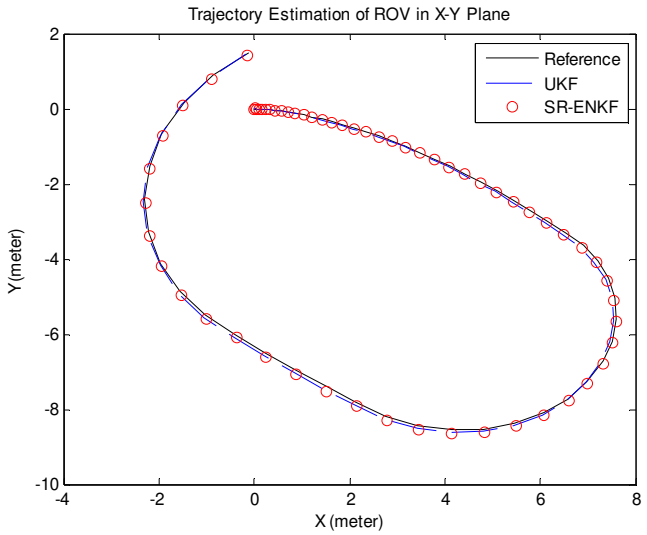

Fig. 4. Comparison of trajectory estimation in the *XY* plane.

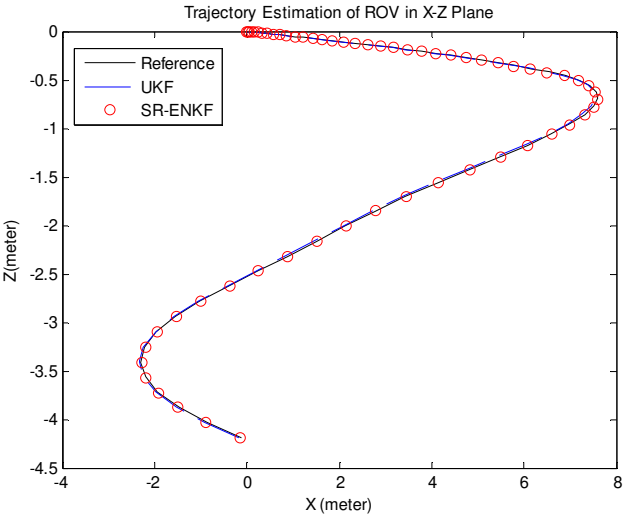

Fig. 5. ROV turning and diving trajectory estimation on the *XYZ* plane by UKF and EnKF-SR with 100 ensemble size.

Figure 7 shows how the ROV follows the trajectory made in the *XY* and *XZ* planes for diving and turning motions. Both methods have high accuracy by not exceeding the design criteria of a maximum position error of less than 2%. Generating 300 ensembles produces an error in the *XY* plane of about 0.09% for the SR-EnKF and 0.32% for the UKF. As can be seen in Table III, the error of the EnKF-SR in each position is smaller than the UKF by about 0.23%.

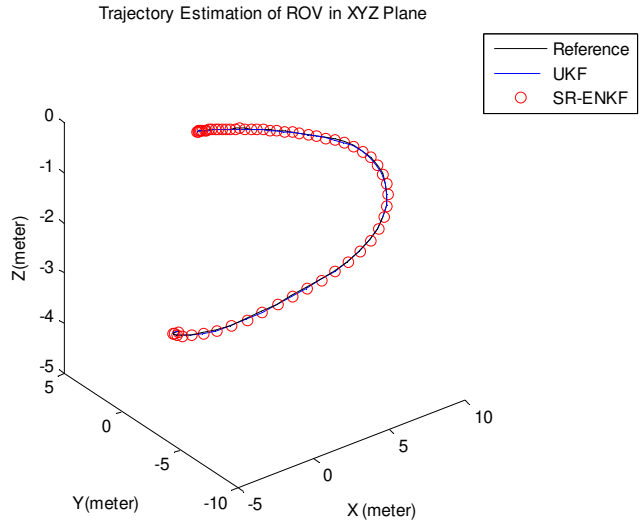

Fig. 6. ROV turning and diving trajectory estimation on the *XYZ* plane by UKF and EnKF-SR with 100 ensemble size.

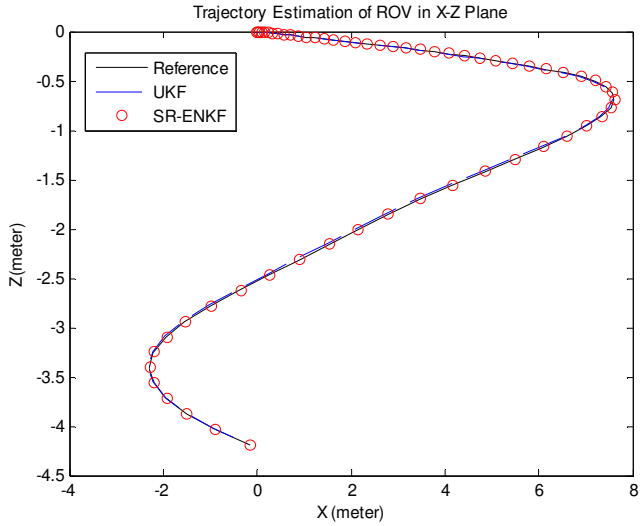

Fig. 8. Estimation of ROV turning and diving trajectories on the *XZ* plane using 300 ensemble size.

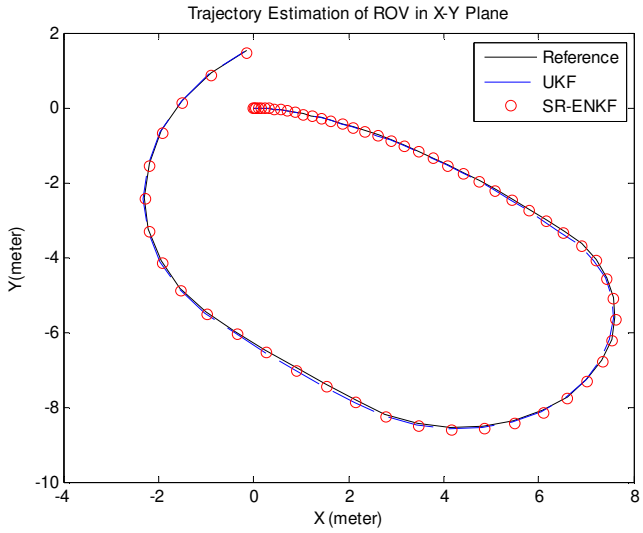

Fig. 7. Estimation of ROV turning and diving trajectories on the *XY* plane.

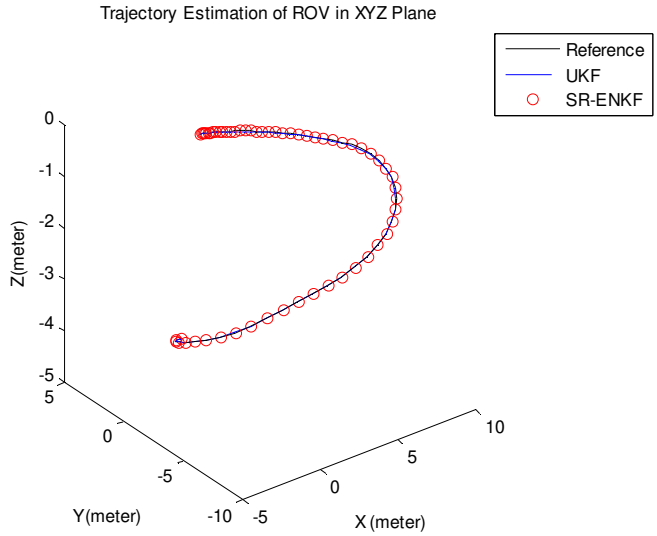

Fig. 9. Trajectory estimation of ROV turning and diving trajectories on the *XYZ* plane using 300 ensemble size.

The trajectory in the *XYZ* plane is a combination of the trajectories made in the *XY* and *XZ* planes displayed in a three-dimensional plane. In the *XYZ* plane, the ROV follows a trajectory where the ROV moves around and dives. In Figure 7, the ROV also follows the trajectory by diving. The ROV can follow the trajectory in both the *XY* and *XZ* planes because the RMSE obtained for motion and rotation is very small. The RMSE of translational and rotational motions is influenced by the calculation of the hydrodynamic coefficients. The suitability of the procedure in determining the value of the hydrodynamic coefficient can reduce the position deviation error. In Table III, we can observe the comparison of position error values using the EnKF-SR and UKF methods.

TABLE III. COMPARISON ROV TRAJECTORY ESTIMATION ERROR OF ENKF-SR AND UKF

	SR-EnKF with 100 ensemble size	**UKF**	**SR-EnKF with 300 ensemble size**	**UKF**
X position	0.0015734	0.0080213	0.0010774	0.0065621
Y position	0.0010736	0.0056837	0.00067014	0.0043569
Z position	0.00045098	0.00050191	0.00027005	0.0019848
XY Motion	0.11%	0.12 %	0.09 %	0.32 %
Simulation	6.324 s	5.721 s	9.586 s	5.891 s

Table III shows a comparison of the simulation results. In terms of accuracy, the SR-EnKF method outperforms the UKF, although it requires a longer simulation time. When comparing the ensemble size, using 300 provides higher accuracy than

100. Overall, the SR-EnKF with ensemble size=300 achieves the best accuracy, but at the cost of increased computation time, as larger ensemble sizes naturally demand more processing.

IV. CONCLUSION

This work presented a comparative study of the Unscented Kalman Filter (UKF) and the Square-Root Ensemble Kalman Filter (SR-EnKF) for nonlinear trajectory estimation of a 6-DoF ROV during diving and turning manoeuvres. The novelty of this research lies in the application of the SR-EnKF with square-root updates to underwater vehicle dynamics, demonstrating its advantages in accuracy and numerical stability compared to the widely used UKF. Simulation results showed that SR-EnKF with ensemble size = 300 achieved the lowest XY error of 0.09%, outperforming UKF on the cost of requiring longer computation time. These findings extend previous works that primarily applied UKF to AUV/ROV navigation, by highlighting that ensemble-based approaches, particularly SR-EnKF, can yield superior accuracy under the same dynamical models and noise assumptions. In practice, the SR-EnKF provides the most precise trajectory estimates, while UKF remains attractive for real-time operations with limited computational resources. Future research will build on this contribution by testing the system robustness against environmental disturbances and validating the approach in experimental field trials.

ACKNOWLEDGMENT

The authors would like to thank LPPM-Universitas Nahdlatul Ulama Surabaya (UNUSA) for their support in providing the facility for this research. Additionally, gratitude is extended to the Centre of Research and Innovation Management of Universiti Teknikal Malaysia Melaka (UTeM) for sponsoring the publication fees under the Tabung Penerbitan CRIM UTeM.

REFERENCES

[1] D. Zhang, B. Zhao, Y. Zhang, and N. Zhou, "Numerical simulation of hydrodynamics of ocean-observation-used remotely operated vehicle," *Frontiers in Marine Science*, vol. 11, Apr. 2024, https://doi.org/10.3389/fmars.2024.1357144.

[2] R. Śmierzchalski and M. Kapczyński, "Autonomous Control of the Underwater Remotely Operated Vehicle in Collision Situation with Stationary Obstacle," *Polish Maritime Research*, vol. 29, no. 4, pp. 45–55, Dec. 2022, https://doi.org/10.2478/pomr-2022-0043.

[3] X.-R. Huang and L.-B. Chen, "An underwater explorer remotely operated vehicle: Unraveling the secrets of the ocean," *IEEE Potentials*, vol. 42, no. 3, pp. 31–36, Feb. 2023, https://doi.org/10.1109/MPOT.2022.3233713.

[4] Y. Cao, B. Li, Q. Li, A. A. Stokes, D. M. Ingram, and A. Kiprakis, "A nonlinear model predictive controller for remotely operated underwater vehicles with disturbance rejection," *IEEE Access*, vol. 8, pp. 158622–158634, Jan. 2020, https://doi.org/10.1109/access.2020.3020530.

[5] K. L. Walker *et al.*, "Experimental Validation of Wave Induced Disturbances for Predictive Station Keeping of a Remotely Operated Vehicle," *IEEE Robotics and Automation Letters*, vol. 6, no. 3, pp. 5421–5428, Jul. 2021, https://doi.org/10.1109/LRA.2021.3075662.

[6] M. I. Fadhok, B. Pramujati, and H. Nurhadi, "Design of sliding mode control for maneuver autonomous surface vehicle using genetic algorithm," *AIP Conference Proceedings*, vol. 2927, no. 1, Mar. 2024, Art. no. 040009, https://doi.org/10.1063/5.0196208.

[7] K. Hasan *et al.*, "Oceanic Challenges to Technological Solutions: A Review of Autonomous Underwater Vehicle Path Technologies in Biomimicry, Control, Navigation, and Sensing," *IEEE Access*, vol. 12, pp. 46202–46231, 2024, https://doi.org/10.1109/ACCESS.2024.3380458.

[8] J. Neira, C. Sequeiros, R. Huamani, E. Machaca, P. Fonseca, and W. Nina, "Review on unmanned underwater robotics, structure designs, materials, sensors, actuators, and navigation control," *Journal of Robotics*, vol. 2021, pp. 1–26, Jul. 2021, https://doi.org/10.1155/2021/5542920.

[9] A. Topini and A. Ridolfi, "Probabilistic Particle Filter Anchoring (PPFA): A Novel Perspective in Semantic World Modeling for Autonomous Underwater Vehicles With Acoustic and Optical Exteroceptive Sensors," *IEEE Journal of Oceanic Engineering*, vol. 50, no. 2, pp. 1065–1086, Apr. 2025, https://doi.org/10.1109/JOE.2024.3492537.

[10] M. E. Hanbaly, S. Iacoponi, A. Infanti, C. Stefanini, G. de Masi, and F. Renda, "Inverse Dynamics Modeling as a State Estimation Aid for Underwater Robots Navigation," *IEEE Access*, vol. 12, pp. 159214–159225, 2024, https://doi.org/10.1109/ACCESS.2024.3487495.

[11] H. Nurhadi, T. Herlambang, and D. Adzkiya, "Trajectory Estimation of Autonomous Surface Vehicle using Square Root Ensemble Kalman Filter," in *2019 International Conference on Advanced Mechatronics, Intelligent Manufacture and Industrial Automation (ICAMIMIA)*, Batu, Indonesia, Jul. 2019, pp. 325–328, https://doi.org/10.1109/ICAMIMIA47173.2019.9223354.

[12] T. Herlambang, D. Rahmalia, A. Suryowinoto, F. Yudianto, F. A. Susanto, and M. Y. Anshori, "H-infinity for autonomous surface vehicle position estimation," *Journal of Physics Conference Series*, vol. 2157, no. 1, Jan. 2022, Art. no. 012022, https://doi.org/10.1088/1742-6596/2157/1/012022.

[13] P. Li *et al.*, "An efficient PSO-based AUV global path planning method incorporating with the positioning uncertainty-driven cost functions of both collision and terrain complexity," *Ocean Engineering*, vol. 336, Sep. 2025, Art. no. 121695, https://doi.org/10.1016/j.oceaneng.2025.121695.

[14] W. Liu *et al.*, "Underwater remotely operated vehicle control system with optimized PID based on improved particle swarm optimization," *Desalination and Water Treatment*, vol. 314, pp. 322–329, Dec. 2023, https://doi.org/10.5004/dwt.2023.30037.

[15] F. F. Sørensen, M. Von Benzon, S. Pedersen, J. Liniger, K. Schmidt, and S. Klemmensen, "Experimental filter comparison of an acoustic positioning system for unmanned underwater navigation," *IFAC-PapersOnLine*, vol. 55, no. 36, pp. 25–30, Jan. 2022, https://doi.org/10.1016/j.ifacol.2022.11.328.

[16] Y. Muratoglu and A. Alkaya, "Unscented Kalman Filter based State of Charge Estimation for the Equalization of Lithium-ion Batteries on Electrical Vehicles," *Engineering Technology & Applied Science Research*, vol. 9, no. 6, pp. 4876–4882, Dec. 2019, https://doi.org/10.48084/etasr.3111.

[17] T. A. Eldamaty and M. M. Helal, "Optimizing GPS kinematic accuracy by employing the Kalman Filter technique, case study: Mecca - Medina Highway," *Engineering Technology & Applied Science Research*, vol. 15, no. 3, pp. 22301–22305, Jun. 2025, https://doi.org/10.48084/etasr.10528.